Available online at www.sciencedirect.com
SCIENCE DIRECT®
Applied Catalysis A: General 266 (2004) 155–162
APPLIED CATALYSIS A: GENERAL
www.elsevier.com/locate/apcata

Modelling the activity–stability pattern of Ni/MgO catalysts in the pre-reforming of *n*-hexane

Francesco Arena*, Giuseppe Trunfio, Emanuele Alongi, Davide Branca, Adolfo Parmaliana

Dipartimento di Chimica Industriale e Ingegneria dei Materiali, Università degli Studi di Messina, Salita Sperone 31, I-98166 S. Agata Messina, Italy

Received 30 October 2003; received in revised form 4 February 2004; accepted 4 February 2004

Available online 15 April 2004

Abstract

The activity–stability pattern of a 19 wt.% Ni/MgO catalyst in the pre-reforming (*T*, 450 °C; *P*, 10 bar) of *n*-hexane with steam (S/C, 1.5–3.5) in absence and presence of H_2 (H/C, 2) has been investigated. Deactivation profiles of the kinetics of CH_4 and CO/CO_2 formation indicate that the activity, selectivity and stability are closely related. Hydrogenation of carbon species to methane is a critical step involving the occurrence of coking in the pre-reforming of hexane. Thermodynamic analysis of the outlet reaction stream signals that the net coking rate depends upon the relative kinetics of carbon methanation (MET, $C + 2H_2 \rightleftarrows CH_4$) and gasification/water–gas-shift (GAS, $C + H_2O \rightleftarrows H_2 + CO$; WGS, $CO + H_2O \rightleftarrows CO_2 + H_2$) reactions, while negligible appears the contribution of the Bouduard reaction path (DISP, $2CO \rightleftarrows C + CO_2$).

Keywords: Pre-reforming; *n*-Hexane; Steam; Ni/MgO catalyst; Activity; Stability; Kinetics; Deactivation; Coking

1. Introduction

Hydrogen is nowadays one the most important chemical finding an extensive use in a variety of industrial processes going from hydrocracking–hydrotreating in oil refining, to fine chemicals production and also as raw material for ammonia and methanol synthesis [1–5]. Apart from latter, the major users of hydrogen are currently the refineries consuming ca. 85% of the total amount produced worldwide, most of which (ca. 65% in US refineries) is available from the catalytic reforming of naphtha [1]. The remainder supply is met by auxiliary production facilities; mostly steam reforming (SR) processes, satisfying ca. 90% of the actual extra hydrogen demand [1,2]. However, this scenario is destined to an abrupt change in the next future for two main reasons [3]: first, the need to reduce progressively the aromatics' content in gasoline, essentially through a lowering of the catalytic reforming severity, will lead to a decreased hydrogen production [1,2]; and second, the expected breakthrough in the fuel market, imposed by the need of cleaner and more efficient fuels (e.g., hydrogen, synthetic gasoline, dimethylether, etc.) produced from natural gas (GTL) rather than from oil, to attain a definitive reduction of NO_x, SO_x and CO_2 emissions from mobile sources [4,5], will impose an extraordinary development of the actual syngas production capacity. On this account, both industrial companies and academic groups are involved since several years in a continuous challenge aimed at upgrading the hydrogen/syngas technology which could result in significant improvements of the overall GTL process economy [1–5]. The exploitation of novel and alternative production routes [3], the engineering of combined and more *energy-effective* reforming technologies [1–3,6] and the enhancement of SR catalysts' performance [6–10] are the pursued routes. In this context, adiabatic pre-reforming constitutes an established technology with recognised economic and operational benefits on the overall syngas production, especially as a tool for revamping older SR plants [1,2,6,11]. Indeed, a pre-reforming unit upstream a tubular reformer allows whatever hydrocarbon feed (NG, LPG, VN) being converted into CH_4 and CO_x at low temperature, typically in 450–550 °C range, with many practical advantages consisting in: (i) an increased produc-

* Corresponding author. Tel.: +39-090-676-5606; fax: +39-090-391-518.
E-mail address: francesco.arena@unime.it (F. Arena).

0926-860X/$ – see front matter © 2004 Elsevier B.V. All rights reserved.
doi:10.1016/j.apcata.2004.02.006

tion capacity with smaller reformer furnaces; (ii) a higher feedstock flexibility; (iii) enhanced SR tubes and catalyst's lifetime; (v) exploitation of innovative process technologies, characterised by lower energy consumption and investment costs [1,2,11]. Ensuring a total conversion of higher hydrocarbons, a pre-reforming unit limits drastically the risk of carbon formation inside tubular reformers allowing, then, SR operations at lower steam-to-carbon (S/C) ratio, with a higher preheat temperature and heat flux and capacity [1,2,6,11–13]. Total elimination of S-containing impurities contributes also to enhance SR catalysts' lifetime [1–3,6,11–13].

Despite of its technological relevance [1,2,6,11–13], a fragmentary knowledge of the basic aspects of the steam reforming of higher hydrocarbons reaction under low (<600 °C) temperature and high pressure conditions exists in literature [6,11–13]. Since earlier works of Rostrup–Nielsen on the steam reforming of C_1–C_7 alkanes on magnesia-supported metal catalysts, leading to the development of the SPARG process [6,12,13], little advances to a deeper knowledge of the title reaction which could result in further improvements of the catalysts' performance have been till now recorded [6,11–13]. Then, mostly semi-empirical models are used to tune process conditions [11] rather than account for the effects of the operating parameters on surface reaction networks [6–13]. Although noble-metal systems feature a high reactivity in the reforming of superior hydrocarbons to hydrogen and carbon oxides [7,9], typical formulations of pre-reforming catalysts include nickel as the active phase [11]. Due to different operating conditions, yet, pre-reforming catalysts are generally richer in Ni loading (50–70 wt.%), bearing rare hearth elements (e.g., La, Sm, Ce, Y, Zr, etc.) as promoters, and are characterised by larger total (SA) and metal surface area (MSA) than counterpart SR ones [6,11]. Loading of the active phase and type of promoters, however, depend upon process characteristics and targets [11].

In earlier papers we documented that Ni/MgO catalysts obtained by an original non-aqueous preparation route exhibit a remarkable performance in both "steam" (H_2O) and "dry" (CO_2) reforming of methane [14–17]. Indeed, hindering the formation of the $NiMgO_x$ solid solution, the above preparation procedure allows a tuning of both physico-chemical and catalytic properties through a proper selection of Ni loading, calcination and reduction treatments [15–17].

Therefore, this paper outlines a series of results concerning the performance of a 19% Ni/MgO catalyst in the pre-reforming of *n*-hexane at 450 °C and 10 bar at steam-to-carbon (S/C) ratio ranging between 1.5 and 3.5 in presence and absence of hydrogen. In the light of a thermodynamic analysis and mathematical modelling of catalytic data, basic insights into reaction network and factors affecting the activity–stability pattern of the Ni/MgO catalyst are achieved.

2. Experimental

The 19.1 wt.% Ni/MgO catalyst (MPF) was prepared by the incipient wetness method using a toluenic solution of nickel acetylacetonate ($Ni(C_5H_7O_2)_2$) and MgO "smoke powder" (UBE Ltd., Japan) as support [14–17]. After impregnation, the catalyst was dried at 80 °C, calcined at 400 °C (16 h) and then pressed (≈400 bar), crushed and sieved to the 40–70 mesh fraction. Before testing the catalyst was subjected to an ex situ pre-reduction in flowing H_2 (6 h) at 650 °C, purging in He flow at the same temperature and a subsequent passivation treatment, consisting in a controlled oxidation by 2% O_2/He pulses (0.25 ml) injection at RT.

Catalyst testing in the pre-reforming of *n*-hexane with steam at 450 °C and 10 bar total pressure was performed using a down-flow fixed bed stainless-steel microreactor (i.d., 6 mm; wall-thickness, 10 mm), timely designed to ensure an adequate heat transfer in the reaction zone. A 25 mg catalyst sample, diluted (1/30 (w/w)) with same-sized carborundum (SiC), was used for testing after an in situ reduction treatment at 450 °C for 1 h under flowing H_2 (100 stp $cm^3\,min^{-1}$). The reaction mixture composition, with and without hydrogen, was set with $C_6H_{14}/H_2O/He/N_2/H_2$ molar ratio percentages equal to 1.8:30.5:36.6:8.0:23.0 and 1.8:30.5:59.6:8.0:0.0, respectively, corresponding to a standard steam-to-carbon ratio (S/C) value of 2.8. The S/C ratio was also varied between 1.5 and 3.5 keeping constant the *n*-hexane flow rate and changing in a balanced way those of H_2O and He. Liquid *n*-C_6H_{14} (*Carlo Erba reagents*, purity >99.9%; S-compounds <0.1 ppm) and bi-distilled water and gaseous (N_2, He, H_2) reactants were fed by HPLC pumps and mass flow controller (He, N_2) respectively, at the total gas flow rate of 286.0 stp $cm^3\,min^{-1}$. The reaction temperature was controlled by a thermocouple put in contact with the catalyst bed, while the reaction stream was analysed on line by a GC equipped with a three columns analytical system and TCD and FID detectors for permanent gases and C_6H_{14} analysis, respectively.

H_2 uptake of "fresh" and "used" catalysts was evaluated by H_2-TPD measurements in the range −80 to 620 °C using Ar as carrier gas (30 stp $cm^3\,min^{-1}$), after an in situ reduction treatment of the samples under H_2 flow at 450 °C for 1 h. The fraction of reduced Ni was evaluated by titration with O_2 pulses at 450 °C in He flow [14–17].

3. Results and discussion

3.1. General aspects

Activity data of the Ni/MgO catalyst in the pre-reforming of *n*-hexane at standard conditions (*T*, 450 °C; *P*, 10 bar; $P_{C_6H_{14}}$, 0.18 bar; P_{H_2O}, 3.0 bar; S/C, 2.8), in terms of *n*-hexane conversion (χ) and product selectivity versus reaction time (t.o.s.), are shown in Fig. 1A. The only detected

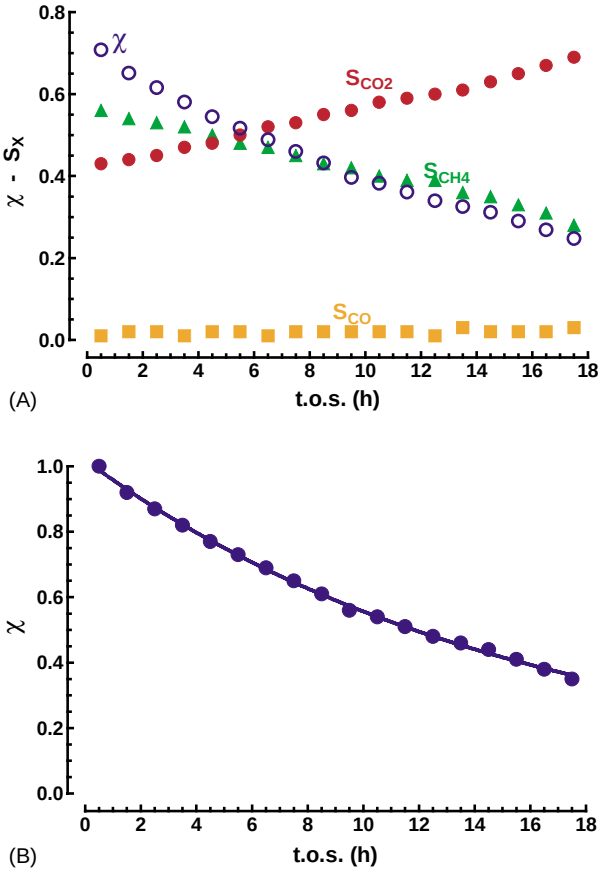

Fig. 1. Pre-reforming of *n*-hexane (*T*, 450 °C; *P*, 10 bar; S/C, 2.8). (A) Conversion (χ) and product selectivity (S_X) vs. t.o.s.; (B) Modelling (Eq. (3)) of the normalised activity α (χ/χ_0) as a function of t.o.s.

C-containing products are CH_4, CO_2 and CO [6,11–13] with a relative distribution which depends on the conversion level during t.o.s. (Fig. 1A). At 30 min, hereafter taken as zero reaction time (t_0), the *n*-hexane conversion is equal to ca. 71% with a CH_4, CO_2 and CO selectivity of ca. 55, 43 and 2%, respectively, indicating that the methanation path is favoured by the high pressure conditions resulting, on the contrary, hindered in steam reforming at atmospheric pressure [7,9]. A significant deactivation of the Ni/MgO catalyst during t.o.s. is, yet, evidenced by a regular and progressive decay in hexane conversion, attaining a final value (after 17.5 h) of ca. 25%, this corresponding to 35% of the initial activity level. Such an activity loss is accompanied by a progressive decrease in CH_4 selectivity counterbalanced by a rise in that to CO_2, reaching final values of 28 and 69%, respectively. Meanwhile, no significant changes in S_{CO} (2–3%) are recorded.

This deactivation trend, handled in terms of normalised conversion rate (α, χ/χ_0), has been inspected by non-linear regression analysis to evaluate the deactivation kinetics and shed lights into the related process(es). As shown in Fig. 1B, the best fit ($r^2 > 0.998$) of experimental "α versus t.o.s." data is attained by an exponential-decay function, pointing to a dependence of deactivation rate which is first-order on

Table 1
H_2 chemisorption data of the "fresh" and "used" (standard run) Ni/MgO catalysts

Sample	α_{NiO} (%)[a]	H_2 upatke (μmol g_{cat}^{-1})	D (%)	MSA (m_{Ni}^2 g_{cat}^{-1})	d_{Ni} (nm)[b]
Fresh	47.1	118.9	16.5	9.3	6
Used	47.2	100.3	13.9	7.8	7

[a] Fraction of reduced NiO determined by O_2 pulses titration at 450 °C.
[b] Average Ni particle size.

conversion:

$$-\frac{d\chi}{dt} = k_{deact}\,\chi \quad (1)$$

Integration at boundary conditions of Eq. (1) leads to the aforesaid exponential relationship

$$\chi = \chi_0\, e^{k_{deac}t} \quad (2)$$

$$\alpha = e^{-k_{deac}t} \quad (3)$$

which provides a deactivation constant (k_{deact}) value equal to 0.0613 h^{-1}. This deactivation trend [18,21] and purity reagents do not match with the occurrence of "selective" poisoning (e.g., by S-compounds) and, then, "fresh" and "used" catalysts were characterised by H_2 chemisorption and TGA–DSC measurements in order to ascertain the occurrence of sintering and/or fouling phenomena, respectively. Namely, comparing H_2 uptakes of "fresh" and "used" MPF samples (Table 1), it is evident that a ca. 15% decrease in MSA cannot be in any case related with the 65% activity loss recorded at the end of run. On the other hand, TGA–DSC analysis (Fig. 2) denotes a high concentration of carbon on the "used" catalyst (ca. 50%) with a related broad eso-peak, centred at ca. 600 °C, index of a poor reactivity of coke deposits [18–20]. According to literature data, these would be constituted by "inert" C_β agglomerates coming from polymerisation and ageing of "reactive" C_α atomic species generated by hexane decomposition [18–20].

The effects of catalyst deactivation on the functionalities driving CH_4, CO and CO_2 formation can be evaluated from

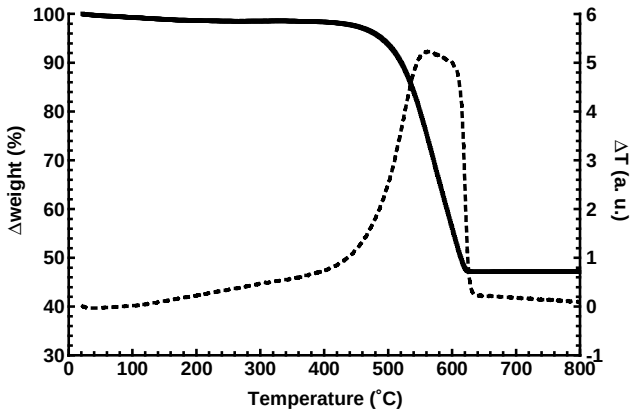

Fig. 2. Pre-reforming of *n*-hexane (*T*, 450 °C; *P*, 10 bar; S/C, 2.8). TGA–DSC data of the "used" catalyst (after 17.5 h t.o.s.).

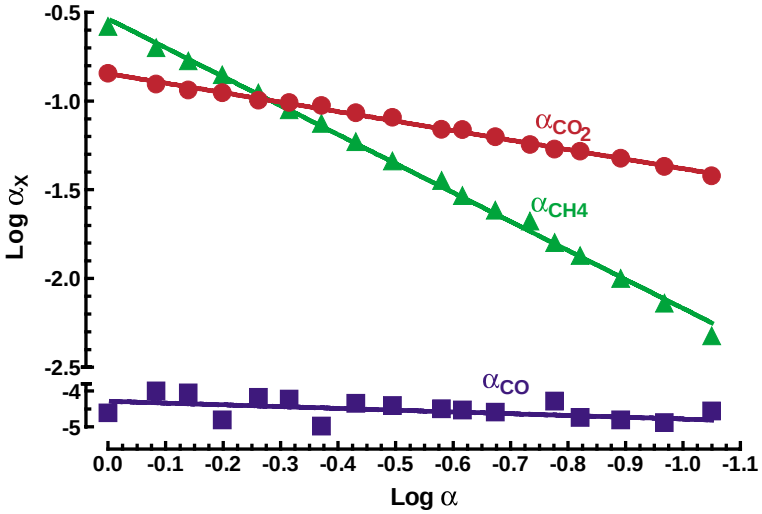

Fig. 3. Pre-reforming of *n*-hexane (*T*, 450 °C; *P*, 10 bar; S/C, 2.8). Relationship between the relative rate of CH_4 (α_{CH_4}), CO_2 (α_{CO_2}) and CO (α_{CO}) formation and normalised activity (α, χ/χ_0).

the "log-plot" of the relative rate (e.g., the ratio between rate at t and t_0 time) of CH_4 (α_{CH_4}), CO_2 (α_{CO_2}) and CO (α_{CO}) formation against the normalised rate of *n*-hexane conversion (α, χ/χ_0). As shown in Fig. 3, the occurrence of quite accurate straight-line relationships allows taking the relative slope as a measure of the effect of catalyst deactivation on the various functionalities and/or vice versa. With a slope value (-1.6 ± 0.1) more than threefold larger than those of α_{CO} (0.5 ± 0.1) and α_{CO_2} (0.5 ± 0.1) then, α_{CH_4} signals a major impact of the methanation functionality on the pre-reforming activity of the Ni/MgO system [6,12,13,19,20]. Considering the absence of any C_2–C_5 hydrocarbon in the outlet stream, a simplified description of the reaction network is possible on the basis of the following irreversible (i, ix) and reversible (ii–viii) surface steps [8,11–13,19–22]:

$$C_6H_{14} + n^* \xrightarrow[K_{H_2O}]{k_{CRK}} (6-m)C_{\alpha(s)} + mCH_{x(s)} + \left[\frac{14-x}{2}\right]H_{2(g)} \quad \text{(i)}$$

$$H_2O + p^* \rightleftarrows H_{2(g)} + O_{(s)} \quad \text{(ii)}$$

$$H_2 + 2^* \underset{k_{GAS}}{\overset{K_{H_2}}{\rightleftarrows}} 2H_{(s)} \quad \text{(iii)}$$

$$C_{\alpha(s)} + O_{(s)} \underset{k_{MET}}{\overset{k_{GAS}}{\rightleftarrows}} CO_{(s)} + \left(\frac{n}{6} + m - q\right)^* \quad \text{(iv)}$$

$$C_{\alpha(s)} + 4H_{(s)} \rightleftarrows CH_{4(g)} + \left(\frac{n}{6} + 4 - t\right)^* \quad \text{(v)}$$

$$CO_{(s)} + O_{(s)} \underset{K_{CO_2}}{\overset{k_{WGS}}{\rightleftarrows}} CO2_{(s)} + (m + q - s)^* \quad \text{(vi)}$$

$$CO_{2(s)} \rightleftarrows CO_{2(g)} + s^* \quad \text{(vii)}$$

$$CH_{4(s)} \underset{k_{cok}}{\overset{K_{CH_4}}{\rightleftarrows}} CH_{4(g)} + t^* \quad \text{(viii)}$$

$$zC_{\alpha(g)} \rightarrow C_\beta(\text{encapsulating} + \text{wiskers}) - w^* \quad \text{(ix)}$$

This confirms a kinetic dependence of the methanation path (MET, v) on concentration of (available) active sites (*) much higher than those of GAS (iv) and WGS (vi) reactions [6,12,13,18–20]. Thus, according to experimental data, the much steeper decay of the methanation functionality with catalyst deactivation (Fig. 3) can be reasonably ascribed to a more pronounced decrease in the $H_{(s)}/C_{\alpha(s)}$ ratio than $O_s/C_{\alpha(s)}$ one [6,12,13,18–20]. In fact, resulting the net coking rate from the rate balance

$$r_{COK} = r_{CRK} - [r_{MET} + (r_{GAS} + r_{WGS})] \quad (4)$$

it is easy to speculate that coking process and surface functionalities are closely related, each affecting the others depending upon the relative effect and reliance on active sites.

3.2. Effects of the S/C ratio and H_2 feeding on the activity–selectivity–stability pattern

The influence of steam on the catalytic behaviour of the Ni/MgO system has been evaluated by performing two other tests at S/C ratio of 1.5 and 3.5. Data at S/C equal to 1.5 (A), 2.8 (B) and 3.5 (C) are comparatively shown in Fig. 4 in terms of normalised activity and relative rate of CH_4, CO_2 and CO formation against t.o.s., while the initial (t_0) values of conversion, product selectivity and reaction rate along with the values of k_{deact} and the amount of coke determined by TGA–DSC analysis of the "used" catalysts, are summarised in Table 2. An increase of the S/C ratio from 1.5 (Fig. 4A) to 3.5 (Fig. 4C) implies a regular rise of the conversion level (Table 2) pointing thus to a positive dependence, though lower than first-order, of reaction kinetics on P_{H_2O} [6,11]. This result compares with the negative-order dependence of pre-reforming kinetics on P_{H_2O} [11], though it must be stressed that L–H equations in literature refer

Table 2
Initial activity data (t_0, 30 min), deactivation kinetic constant and amount of carbon deposits (after 17.5 h of t.o.s.) of the Ni/MgO catalyst in the pre-reforming of n-C_6H_{14} at various S/C ratio (T, 450 °C; P, 10 atm)

S/C	$\chi_{C_6H_{14}}$ (%)	$Rate_{C_6H_{14}}$ ($\mu mol\,s^{-1}\,g_{cat}^{-1}$)	S_{CH_4} (%)	S_{CO_2} (%)	S_{CO} (%)	k_{deact} (h^{-1})	w_{carbon} ($g\,g_{cat}^{-1}$)
1.5	52.6	82.0	54.9	42.6	2.5	0.114	1120
2.8	70.8	110.3	55.4	43.1	1.5	0.061	960
3.5	82.9	129.2	56.2	42.5	1.3	0.049	890

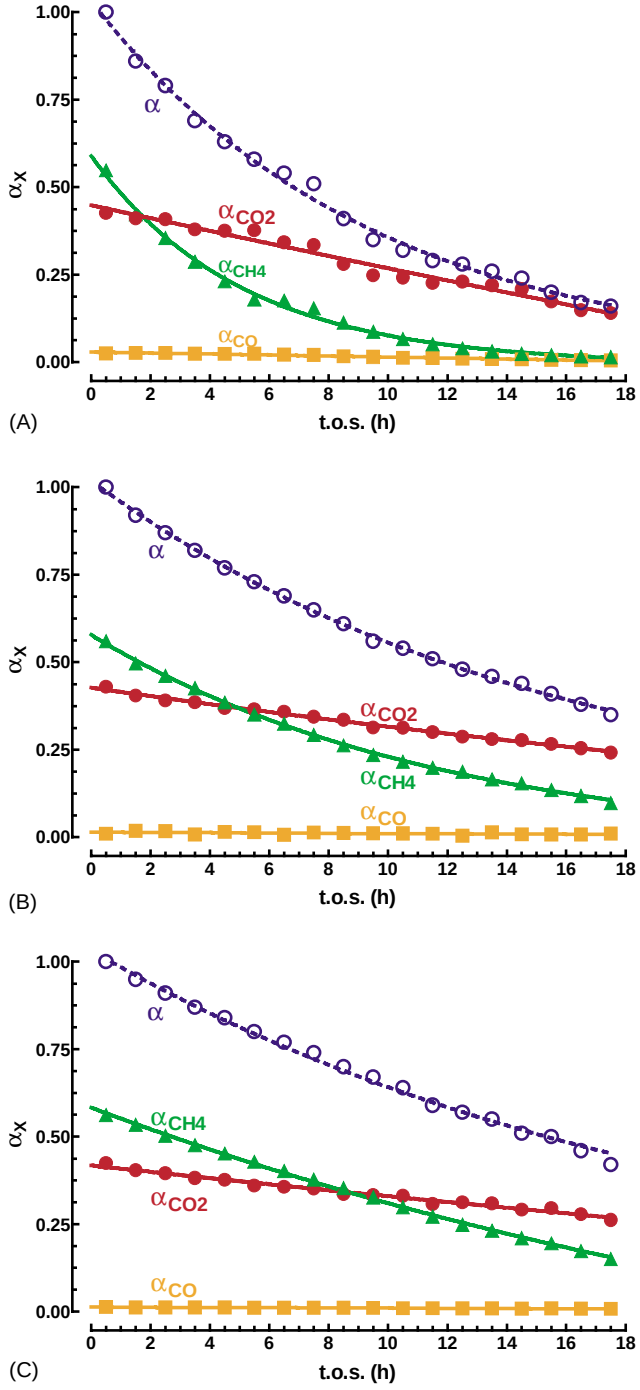

Fig. 4. Pre-reforming of n-hexane (T, 450 °C; P, 10 bar). Normalised activity (α, χ/χ_0) and relative rate of CH_4 (α_{CH_4}), CO_2 (α_{CO_2}) and CO (α_{CO}) formation vs. t.o.s. Effect of the S/C ratio: (A) S/C, 1.5; (B) S/C, 2.8; (C) S/C, 3.5.

to testing in the presence of hydrogen and, thus, when a "competition" effect for active sites by H_2 (reaction iii) and H_2O (reaction ii) determines a negative impact of the last reactant on reaction kinetics [7,8,11,18–20]. In spite of negligible changes in selectivity (Table 2), an improved stability, denoted by a decrease of k_{deact} from 0.114 (S/C, 1.5) to 0.049 h^{-1} (S/C, 3.5), is the major effect of higher S/C ratios. Namely, graphing in a "log-plot" k_{deact} values against the S/C ratio (Fig. 5A), a reliable linear relationship (r^2, 1.00) with a slope value of −0.99 (e.g., $k_{deact} \propto (S/C)^{-1}$) is obtained. This finding clearly addresses the crucial influence of the S/C ratio on deactivation by coking [6,11–13,18–20], as proved by the straight relationship between k_{deact} and weight loss recorded in TGA measurements (Fig. 5B).

At least, the activity–stability pattern of the Ni/MgO catalyst in presence of H_2 feeding (H_2/C, 2; S/C, 2.8) can be evaluated from data shown in Fig. 6. With reference to standard testing conditions (Fig. 1A), data in Fig. 6 display that H_2 in the feed enables a ca. 25% rise in the initial conversion value (from ca. 71 to 88%) along with a striking change in selectivity, evidenced by an increase of S_{CH_4} from ca. 55 to 98–99% and a corresponding drop in S_{CO} and S_{CO_2} at a same very low level (0.5–1%). Associated to these marked changes in activity and selectivity, yet, the most striking consequence is a quite improved stability involving an activity loss (ca. 10%) much slighter (ca. 65%) than that recorded in absence of hydrogen (after 17.5 h). Evidently, these findings catch the salient aspects of the above reaction scheme, conveying hat a competitive coverage by C_{ads}, O_{ads} and H_{ads} species determine their relative surface abundance and, therefore, the rate of the various surface steps with consequent effects on both reaction and coking kinetics [18,21].

3.3. Thermodynamic evaluations

In the light of above results, a thermodynamic analysis of the outlet stream composition [6,11,18–21] has been devised to shed lights into driving forces to carbon deposition. As cracking of hexane can be considered irreversible [6,18–21], a reliable evaluation of the outlet gas composition evidently lies on the analysis of gasification (GAS), water–gas-shift (WGS), methanation (MET) and Bouduard (DISP) reactions (Table 3) [6–10,13,19]. Namely, substituting the P_x values (from conversion–selectivity data) in the expressions of the relative equilibrium constant, experimental K_{exp} values for MET, GAS/WGS and DISP reactions as a function of t.o.s.

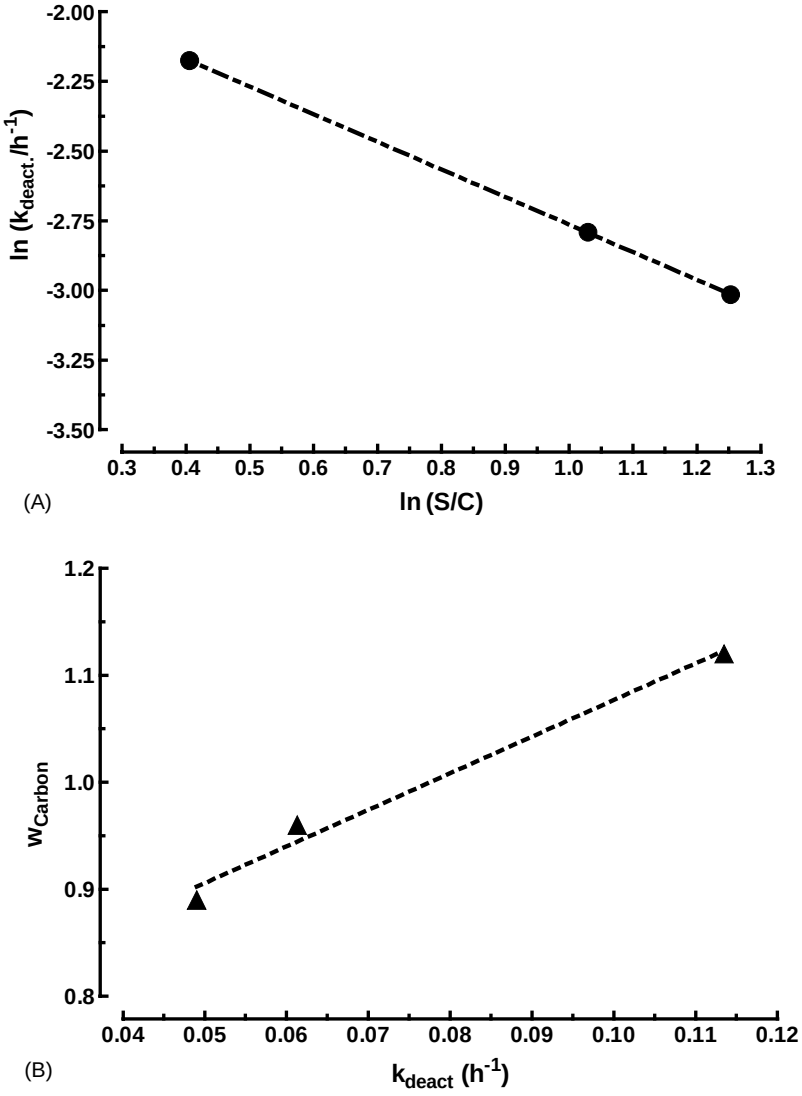

Fig. 5. Pre-reforming of *n*-hexane (*T*, 450 °C; *P*, 10 bar). (A) Log-plot of k_{deact} vs. the S/C ratio; (B) relationship between carbon concentration on the "used" catalysts (TGA–DSC) and k_{deact} at different S/C ratio.

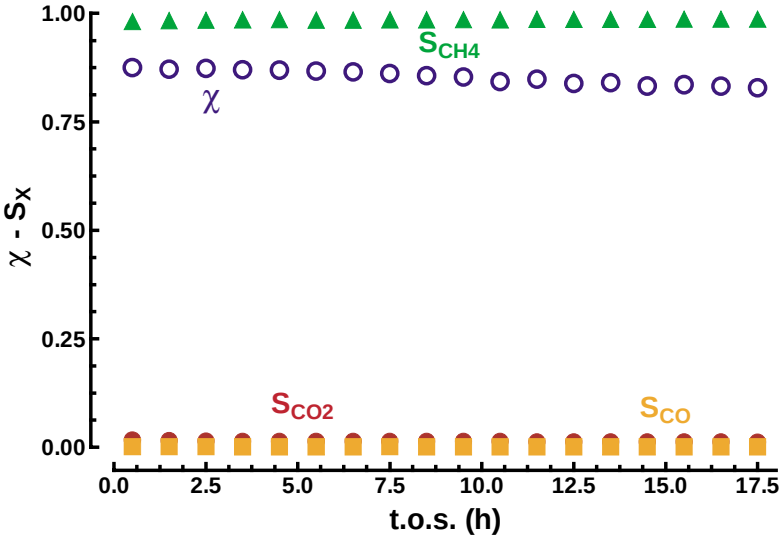

Fig. 6. Pre-reforming of *n*-hexane (*T*, 450 °C; *P*, 10 bar; S/C, 2.8). Effect of H_2 feeding (H_2/C, 2): conversion (χ) and product selectivity (S_X) vs. t.o.s.

Table 3
List of reactions considered for thermodynamic evaluations of catalytic data

Reaction	Stoichiometry	K_P[a]
CRK	$C_6H_{14} \rightarrow 6\ C + 7\ H_2$	–
GAS	$C + H_2O \rightleftarrows CO + H_2$	5.09 E−4
WGS	$CO + H_2O \rightleftarrows CO_2 + H_2$	7.47 E+0
MET	$C + 2H_2 \rightleftarrows CH_4$	5.41 E+1
DISP	$2CO \rightleftarrows C + CO_2$	1.47 E+4

[a] Equilibrium pressure constant values at 450 °C with P_X values in MPa (adapted from reference [13]).

were obtained. Therefore, the ratio (β) between K_{exp} and the corresponding value of the equilibrium constant K_{eq} at 450 °C (Table 3) allows for a reliable evaluation of the effects of the S/C ratio (Fig. 7A-C) and H_2 feeding (Fig. 7D) on the catalyst reactivity. Namely, data shown in Fig. 7 indicate that irrespective of t.o.s. and S/C ratio, WGS is always close to thermodynamic equilibrium conditions, being characterised by β_{WGS} values comprised between 0.6 and 1.0. On the contrary, gasification ($\beta_{GAS} \approx 0.5$) but, mostly, methanation (β_{MET}, 0.2–0.05) are always under kinetic control, their lower rate with respect to cracking being the driving force to carbon deposition and growth [6,19–22]. On the other hand, a β_{DISP} always larger than one (Fig. 7) compels apposite considerations, since a $[P_{CO_2}/(P_{CO})^2]$ value larger than that allowed by thermodynamics really points to a poor efficiency of the catalyst in promoting the carbon gasification by reaction with CO_2 (DISP), mostly coming from WGS. Further, while β_{GAS} and β_{MET} decrease always with t.o.s. like relative activity (α), β_{DISP} rises according to a specular trend (Fig. 7) indicating a direct but different influence of the coking process on all these reactions. In particular, considering that surface carbon is a common intermediate in all the above reaction steps (see reaction scheme), these results would be diagnostic of a progressive decrease in the reactivity of surface carbon (C_s) in concomitance with ageing of coke deposits (e.g., $C_\alpha \rightarrow C_\beta$) [6,11,18–21]. In agreement with literature data [6,11,18–21], a rather different influence of catalyst fouling on the various functionalities is then expected [20]. Indeed, despite of a considerable decrease in the availability of metal surface area induced by the growth of gum-like carbonaceous deposits, Jackson et al. found that a Ni/Al_2O_3 catalyst retains a rather high activity towards

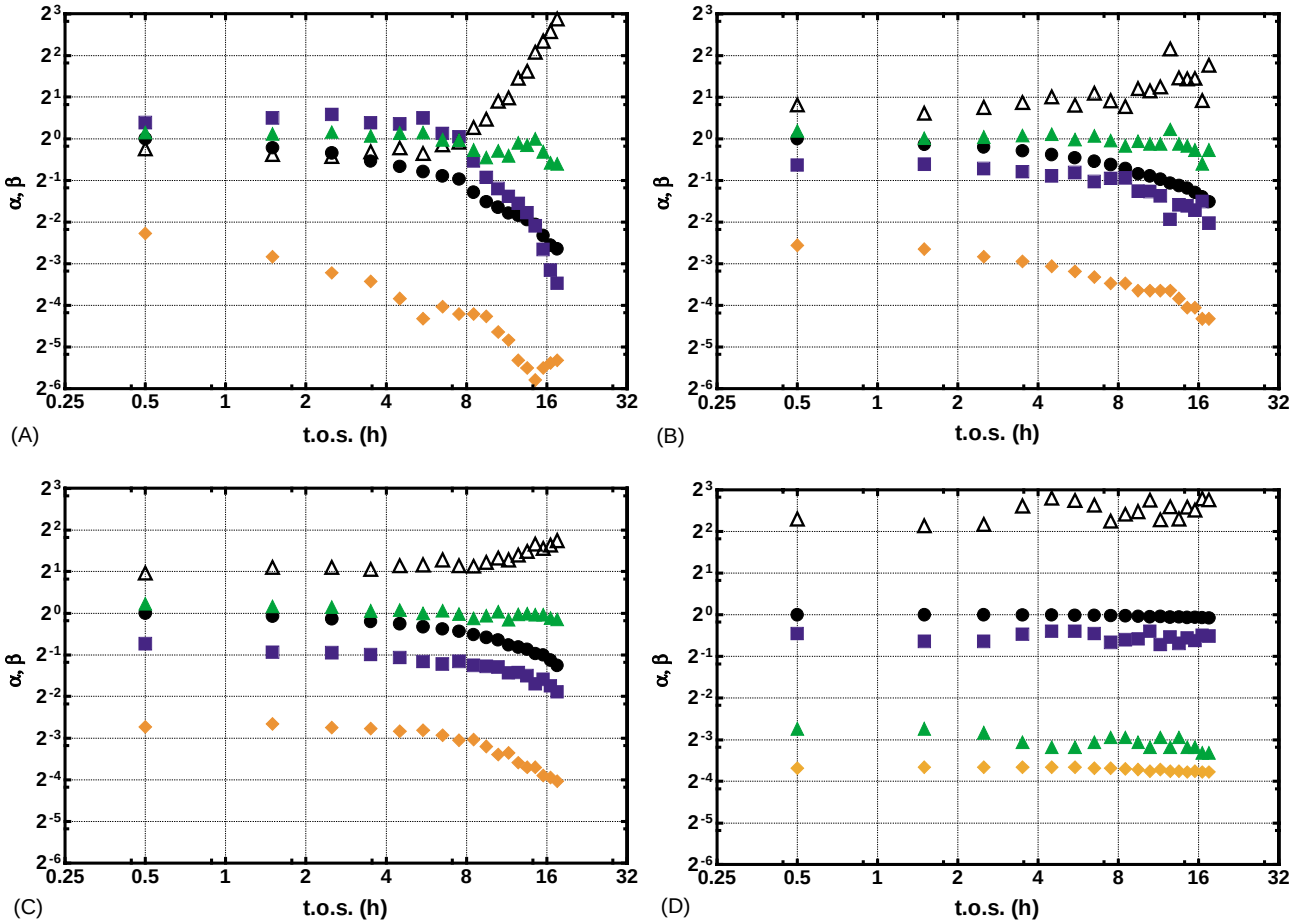

Fig. 7. Pre-reforming of *n*-hexane (*T*, 450 °C; *P*, 10 bar). Effect of the S/C ratio and H_2 feeding. α and β values of GAS, WGS, MET and DISP reactions vs. t.o.s.: (A) S/C, 1.5; H_2/C, 0; (B) S/C, 2.8; H_2/C, 0; (C) S/C, 3.5; H_2/C, 0; (D) S/C, 2.8; H_2/C, 2. Legend: (●) α; (▲) β_{WGS}; (△) β_{BOUD}; (■) β_{GAS}; (◆) β_{MET}.

the scrambling of C-atoms with isotope-labelled ^{14}CO and $^{14}CO_2$ and surface carbon gasification [20]. On the other hand, Bartholomew emphasised that methanation and steam reforming functionalities of Ni catalysts are closely related on the basis of the activation energy values [19], while Rostrup–Nielsen stressed that hydrogenolysis and steam reforming reactions share most of the surface steps, requiring also analogous ensembles (*n*, 2.5–2.7) of active sites [6]. In this context, it is easily to speculate that H_2 feeding strongly promotes the activity and stability because of the enhancement of the methanation functionality enabled by a high availability of activated H atoms (H_s) at the catalyst surface. In turn, hydrogen prevents the formation of "encapsulating" carbon responsible of deactivation [6,18–22] while, limiting the water splitting (reaction ii), it also implies a drop in both CO and CO_2 selectivity (Fig. 6). In other words, literature data well match with experimental findings, conveying that hydrogenation is a crucial step, its kinetics controlling activity, selectivity and stability against coking in the pre-reforming reaction. Whereas, an extensive coverage of active sites at steady-state by C_s, O_s and H_s species hinders the backward DISP until getting "C–CO–CO_2" equilibrium conditions [18,23]. This hypothesis is confirmed by two additional evidences: i) the initial β_{DISP} values rise with S/C ratio and H_2 feeding (Fig. 7), resulting the highest (>4) in latter case, thus in concomitance with an extensive saturation of active sites by H_s and/or O_s species and ii) the (positive) deviation of β_{DISP} rises with the deactivation level (Fig. 7), resulting the most pronounced at the lowest S/C ratio (Fig. 7A), thus when a faster coking rate causes the largest surface coverage by C_s species. A rising stability of surface carbon during t.o.s. [6,11,18–23] concur further to the enhanced displacement of out-of-equilibrium conditions of MET, GAS and DISP reactions with t.o.s. (Fig. 7).

4. Conclusions

The activity–stability pattern of the Ni/MgO catalyst in the pre-reforming of *n*-C_6H_{14} with steam at 450 °C and 10 bar has been addressed.

The effects of steam-to-carbon ratio and H_2 feeding on reaction and deactivation kinetics have been highlighted.

In particular, the onset of experimental findings can be summarised as follows:

- In absence of H_2, the deactivation rate of the Ni/MgO catalyst follows a first-order dependence on activity, resulting in an *exponential decay* with t.o.s. The *deactivation constant* value is *inversely* proportional to the S/C ratio;
- Thermodynamic analysis of the outlet stream composition indicates that the relative kinetics of CRK and MET + GAS/WGS reactions control the coking rate. Methanation is a critical step responsible of coking in absence of H_2;
- Hydrogen feeding strongly promotes the methanation activity speeding up the overall reaction kinetics which results in a quite improved stability of the Ni/MgO catalyst against coking phenomena.

References

[1] B.J. Cromarty, C.W. Hooper, Increasing the throughput of an existing hydrogen plant, Int. J. Hydr. En. 22 (1997) 17–22.
[2] A.M. Aitani, Processes to enhance refinery-hydrogen production, Int. J. Hydr. En. 21 (1996) 267–271.
[3] J.L.G. Fierro, M.A. Peña, J.P. Gómez, New catalytic routes for syngas and hydrogen production, Appl. Catal. A: Gen. 144 (1996) 7–57.
[4] W.J. Piel, Transportation fuels of the future, Fuel Proc. Technol. 71 (2001) 167–179.
[5] S. Nagase, S. Takami, A. Hirayama, Y. Hirai, Development of a high efficiency substitute natural gas production process, Catal. Today 45 (1998) 393–397.
[6] J.R. Rostrup-Nielsen, I. Alstrup, Innovation and science in the process industry: steam reforming and hydrogenolysis, Catal. Today 53 (1999) 311–316.
[7] T. Suzuki, H. Iwanami, T. Yoshinari, Steam reforming of kerosene on Ru/Al_2O_3 catalyst to yield hydrogen, Int. J. Hydr. En. 25 (2000) 119–126.
[8] Q. Ming, T. Healey, L. Allen, P. Irving, Steam reforming of hydrocarbon fuels, Catal. Today 77 (2002) 51–64.
[9] X. Wang, R.J. Gorte, A study of steam reforming of hydrocarbon fuels on Pd/ceria, Appl. Catal. A: Gen. 224 (2002) 209–218.
[10] A. Ayabe, H. Omoto, T. Utaka, R. Kikuchi, K. Sasaki, Y. Teraoke, K. Educhi, Catalytic autothermal reforming of methane and propane over supported metal catalysts, Appl. Catal. A: Gen. 241 (2003) 261–269.
[11] T.S. Christensen, Adiabatic prereforming of hydrocarbons—an important step in syngas production, Appl. Catal. A: Gen. 138 (1996) 285–309.
[12] J.R. Rostrup-Nielsen, Activity of nickel catalysts for steam reforming of hydrocarbons, J. Catal. 31 (1973) 173–181.
[13] J.R. Rostrup-Nielsen, in: J.R. Andersen, M. Boudart (Eds.), Catalysis, Science and Technology, vol. 5, Springer, Berlin, 1983, p. 1.
[14] F. Arena, B.A. Horrell, D.L. Cocke, A. Parmaliana, N. Giordano, Magnesia-supported nickel catalysts. Part I. Factors affecting the structure and morphological properties, J. Catal. 132 (1991) 58–67.
[15] A. Parmaliana, F. Arena, F. Frusteri, S. Coluccia, L. Marchese, G. Martra, A. Chuvilin, Magnesia-supported nickel catalysts. Part II. Surface properties and reactivity in methane steam reforming, J. Catal. 141 (1993) 34–47.
[16] F. Frusteri, L. Spadaro, A. Chuvilin, F. Arena, A TEM study of carbon genesis on bare and K-doped Ni/MgO catalysts during dry-reforming of methane, Carbon 40 (2002) 1063–1070.
[17] F. Frusteri, F. Arena, G. Calogero, T. Torre, A. Parmaliana, K-enhanced stability of Ni/MgO catalysts in the dry reforming of methane, Catal. Commun. 2 (2001) 49–56.
[18] J.B. Butt, E.E. Petersen, Activation, Deactivation and Poisoning of Catalysts, Academic Press, San Diego, CA, USA, 1998, pp. 27–82.
[19] C.H. Bartholomew, Carbon deposition in methanation and steam reforming, Catal. Rev. Sci. Eng. 24 (1982) 67–112.
[20] J.G. McCarty, H. Wise, Hydrogenation of surface carbon on alumina-supported nickel, J. Catal. 57 (1979) 406–416.
[21] P. Forzatti, L. Lietti, Catalyst deactivation, Catal. Today 52 (1999) 165–181.
[22] S.D. Jackson, S.J. Thomson, G. Webb, Carbonaceous deposition associated with the catalytic steam-reforming of hydrocarbons over nickel alumina catalysts 70 (1981) 249–263.
[23] M.S. Spencer, On the activation energies of the forward and reverse water gas shift reaction, Catal. Lett. 32 (1995) 9–13.